

CrystEngComm

Accepted Manuscript



This is an *Accepted Manuscript*, which has been through the Royal Society of Chemistry peer review process and has been accepted for publication.

Accepted Manuscripts are published online shortly after acceptance, before technical editing, formatting and proof reading. Using this free service, authors can make their results available to the community, in citable form, before we publish the edited article. We will replace this *Accepted Manuscript* with the edited and formatted *Advance Article* as soon as it is available.

You can find more information about *Accepted Manuscripts* in the [Information for Authors](#).

Please note that technical editing may introduce minor changes to the text and/or graphics, which may alter content. The journal's standard [Terms & Conditions](#) and the [Ethical guidelines](#) still apply. In no event shall the Royal Society of Chemistry be held responsible for any errors or omissions in this *Accepted Manuscript* or any consequences arising from the use of any information it contains.

Simultaneous improvement in afterglow, light yield and energy resolution in CsI:Tl-based scintillators paves the way to its application in computer tomography and high-speed imaging.

Cite this: DOI: 10.1039/c0xx00000x

www.rsc.org/xxxxxx

CsI:Tl⁺,Yb²⁺:Ultra-high light yield scintillator with reduced afterglow

Yuntao Wu,^{a,*} Guohao Ren,^{a,*} Martin Nikl,^b Xiaofeng Chen,^a Dongzhou Ding,^a Huanyin Li,^a Shangke Pan,^a Fan Yang^c

Received (in XXX, XXX) Xth XXXXXXXXX 20XX, Accepted Xth XXXXXXXXX 20XX

DOI: 10.1039/b000000x

Afterglow problem has been preventing CsI:Tl single crystal scintillators from applications in the field of computer tomography and high-speed imaging. We show that Yb²⁺ codoping in CsI:Tl can reduce it at least by one order of magnitude after 50 ms from X-ray cut-off compared to ordinary CsI:Tl. After optimization of the Yb²⁺ and Tl⁺ concentrations, the doubly doped CsI:Tl,Yb crystal exhibits an ultra-high light yield of 90,000±6000 photons/MeV, energy resolution 7.9%@511 keV and low afterglow level of about 0.035% at 80 ms. Simultaneous improvement in afterglow, light yield and energy resolution in CsI:Tl-based scintillators paves the way to its application in computer tomography and high-speed imaging. The physical mechanism and role of ytterbium ions in afterglow suppression were proposed.

Tl-doped cesium iodide was introduced in 1951 as one of the first single crystal scintillators.¹ It shows high light yield 66,000 photons/MeV, scintillation response dominated by 800-1000 ns decay time and an emission band at 550 nm matching well the semiconductor photodetector sensitivity range.² Furthermore, it has medium density (4.53 g/cm³) and higher effective atomic number ($Z_{\text{eff}} = 54$) and allows the fabrication of micro-columnar films. Given its low cost, CsI:Tl materials became widely used for radiological imaging,³ x-ray and gamma ray spectroscopy, homeland security and nuclear medicine applications. However, due to the persistent afterglow in CsI:Tl attributed to thermal ionization of trapped electrons (Tl₀) followed by radiative recombination with trapped holes [$V_{\text{KA}}(\text{Tl}^+)$],⁴ which causes the pulse pileup in high count-rate applications, its usage in computer tomography (CT) and high-speed imaging applications is disabled.^{5,6} Thus, the way to suppress the afterglow in CsI:Tl has been searched intensively in last two decades.

In general, co-doping by an appropriate ion was found an effective method to suppress the afterglow in scintillators and phosphors as has been shown e.g. in Gd₂O₂S-based or (Y,Gd)₂O₃-based phosphors and optical ceramics, see Ref. 2 and refs. therein. Afterglow in Lu₂SiO₅:Ce (LSO:Ce) scintillator has been soon recognized as a serious limitation⁷ and the Ca²⁺ codoping was found efficient for its suppression^{8,9}. Positive role of Yb²⁺ ions in the afterglow suppression of LSO:Ce was found as well, decreasing it by more than two orders of magnitude, however, at serious expense of the light output.¹⁰ In CsI:Tl scintillators, the afterglow level was effectively reduced by codoping Eu²⁺ and

Sm²⁺ ions.¹¹⁻¹⁴ Nevertheless, the atomistic mechanism of Eu²⁺ and Sm²⁺ functioning is utterly different. Samarium ions introduce a non-radiative recombination channel that decreases the radiative recombination of trapped carriers,¹⁴ but co-doping with europium introduces deep electron traps scavenging electrons from shallow traps associated with thallium, which results in a slower afterglow.¹² However, co-doping with these ions seriously deteriorated the light yield in both cases. Recently, Totsuka et al. claimed that using the Bi³⁺ codoping the afterglow of CsI:Tl can be less than 0.1% after 10 ms without strong decrease of the radioluminescence efficiency under low energy X-ray (less than 30 keV) excitation.¹⁵ However, in the attempt to verify this result, we found that the light yield and energy resolution of Bi-codoped CsI:Tl crystals became much worse even for the lowest Bi concentration of about 0.005 mol% (in the melt).¹⁶

Therefore, despite of the success in the afterglow suppression in CsI:Tl the codoping strategies mentioned above have simultaneously deteriorated the other important scintillation characteristics such as light yield and energy resolution which points to the complex character of scintillation mechanism. Impurities (doped ions) may introduce energy levels in the band gap of the host crystal which interfere with the charge carrier migration and relaxation processes: while the afterglow level is dramatically improved, other scintillation properties such as light yield and energy resolution may be seriously degraded.

The search for codopants which can effectively diminish the delayed radiative recombination (afterglow) at Tl⁺ centres and not deleteriously affect other scintillation properties is the primary goal of this work. Due to the electronic structure similarity between Eu²⁺ and Yb²⁺,¹⁷ the afterglow suppression effect by Yb²⁺ codoping is expected. Thus, in this paper, we study the effects of Yb²⁺ co-doping on the optical and scintillation properties of CsI:Tl, including afterglow level, light yield, energy resolution, and relative scintillation efficiency.

We used vertical Bridgman technique to grow two groups of CsI:Tl,Yb crystals. The crystals referred to as group A are used for screening the effect of Yb²⁺ codoping: CsI:0.078mol%Tl⁺ (further denoted as IT1), CsI:0.078mol%Tl⁺,0.005mol%Yb²⁺ (further denoted as IT2) and CsI:0.078mol%Tl⁺,0.05mol%Yb²⁺ (further denoted as IT3). The other crystals referred to as group B are to further optimize the recipe: CsI:0.156mol%Tl⁺ (further denoted as ST3), CsI:0.156mol%Tl⁺,0.005mol%Yb²⁺ (further

denoted as ST1) and CsI:0.234mol% Ti^+ ,0.005mol% Yb^{2+} (further denoted as ST4). The high-purity CsI (5N), TlI (4N) (both from Chemetall), and YbI_2 (5N) (Aldrich) according to the stoichiometric ratio were loaded in the quartz ampoules and then heated in vacuum to eliminate the residual humidity. The ampoules were maintained at a temperature 100°C above the melting point of cesium iodide for 24 hours to ensure homogeneity of the melt. Then, ampoules were passed through an optimal temperature gradient with a speed of 0.6 mm/h. The resultant boules were 35 mm in diameter and 100 mm in length. All the crystals were transparent and colorless (see inset of Figure 1). The samples used for dopant concentration measurement were cut at the same position along the boule. The actual dopant concentrations in the crystals were measured by Perkin-Elmer ELAN DRC-e Inductively Coupled Plasma Mass Spectrometry (ICP-MS). The measured Ti^+ concentration in crystals are listed in Table 1 and Table 2. Yb concentration was below sensitivity limit of the apparatus (5 ppm) so that the data are not shown here. All samples were clear and uniform, without any visible inclusions or cracks. Two sample dimensions were chosen for measurements. The first one was $\varnothing 25.4 \times 25.4 \text{ mm}^3$ double-faced polished crystals (see inset of Figure 1). These samples were wrapped in Teflon tapes and used for afterglow, pulse height spectra and X-ray excited luminescence spectra measurements. Before these measurements, all wrapped crystals were stored in the dark for at least 24 hrs. The second sample dimension was double-faced polished $5 \times 5 \times 2 \text{ mm}^3$ plate used for the rest of measurements.

The afterglow curves were measured by using a single-shot pulse X-ray excitation (pulse duration of 80 ns). The afterglow profiles were recorded by using 20000 data points taken from the oscilloscope (Tektronix DPO 5104) using a photomultiplier (PMT) tube detection (R669). The afterglow level $\eta(t)$ was calculated as a ratio between the luminescence intensities (I_0) measured during the X-ray irradiation pulse and at the time delay (t) after the irradiation is terminated, namely $\eta(t) = I(t)/I_0 \times 100\%$. The wrapped cylinder group A crystals for light yield measurement were coupled with a Hamamatsu R878-WT1734 series PMT with no optical grease or other coupling material. The crystals were excited with 662 keV gamma rays from ^{137}Cs source located 10 mm from the crystal surface, and then pulse-height spectra were recorded by Digibase multichannel spectrometer. The shaping time and PMT high voltage was fixed at 2 μs and 1050 V, respectively. The natural background spectrum from the crystal was not subtracted.

The wrapped cylinder group B crystals for absolute light yield and energy resolution measurements were coupled with Hamamatsu R1306 PMT with a bi-alkali photo-cathode and a borosilicate glass window. A collimated ^{22}Na source (511keV) was used to excite the samples. The photopeak positions were obtained by a simple Gaussian fit. The light output (LO) is measured by single photo-electron peak calibration. The absolute light yield (LY) was calculated using LO, the emission weighted quantum efficiency (EWQE) of the Hamamatsu R1306 PMT at 550 nm which is of about $5.0 \pm 0.3\%$, and light collection efficiency (LCE) which is assumed to be 1. The specific equation $\text{LY} [\text{photons/MeV}] \approx \text{LO} [\text{photoelectrons/MeV}] / (\text{EWQE} \times \text{LCE})$ was used. Scintillation decay time was measured by the same equipment by tuning the integration time. Scintillation measurements described for group B samples were performed at

Prof. Renyuan Zhu's HEP group in California Institute of Technology.

The radioluminescence spectra without calibration were conducted on an X-ray Excited Luminescence Spectrometer, assembled at Shanghai Institute of Ceramics. The excitation source of this equipment is medical F30III-2 type mobile diagnostic X-ray machine coupled with the 44W plane grating monochromator and Hamamatsu R456 PMT. Optical absorption spectra were recorded on a Varian Cary 5000 spectrophotometer. Photoluminescence decay profiles were recorded on Edinburgh FLS920 fluorescence spectrometer, respectively. All the above described measurements were performed at room temperature.

Figure 1 presents the results of afterglow measurements performed at the group A crystals. The afterglow level of the Yb^{2+} codoped ones decreases by more than one order of magnitude in comparison with Yb^{2+} -free one after 50 ms. Comparing with the Eu^{2+} , Sm^{2+} or Bi^{3+} codopants mentioned above the performance of Yb^{2+} codopant is comparable as it lowers the afterglow level down to 0.041% in comparison with 0.03% for Bi^{3+} ,¹⁵ ~0.03% for Eu^{2+} codopant,¹¹ and ~0.1% for Sm^{2+} .¹³

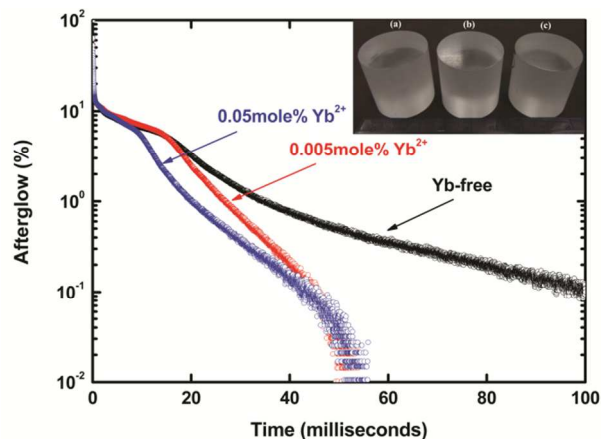


Fig. 1 Afterglow profiles of CsI: Ti^+ , Yb^{2+} group A crystals after X-ray pulse excitation. Inset shows the photograph of double-faced polished group A crystals with different Yb^{2+} concentration: none (a), 0.005% (b), 0.05% (c).

The emission spectra under steady-state X-ray excitation of group A crystals were measured (see supplemental data). In the Yb-doped samples the emission spectrum exhibits similar pattern to that of the Yb-free one.¹¹ After normalization, an interesting phenomenon was noticed: a gradual decrease of relative intensity of the shoulder at 400 nm with increasing Yb^{2+} concentration compared to maximum of the spectrum around 500 nm (defined as 100%) clearly occurs, see Table 1. Integrating the radioluminescence spectra, the relative scintillation efficiency can be compared among the samples. The decreasing trend in Yb-doped samples is obvious and relative reduction is larger than that of relative light yield, see Table 1. Because the emission under steady-state X-ray excitation (scintillation efficiency) includes both the fast scintillation component (measured in light yield) and the slower (delayed) components responsible for the afterglow, it means that the Yb^{2+} codoping is reducing the unwanted slower components. For CsI:Tl, the unwanted slower components (afterglow emission) was ascribed to the delayed Tl-related band

peaking at about 560 nm¹⁸ and 400 nm¹⁹. Due to the strong decrease of the quantum efficiency of the PMT above 500 nm, the true maximum of the emission at 550-560 nm cannot be observed in our uncorrected spectra. In our spectra, the maximum of this emission in our spectra peaks at 500 nm. The cause for the relative decrease of 400 nm shoulder in the emission spectra of Yb-codoped samples will be discussed in the following paragraph. The photoluminescence decay times of CsI:Ti⁺,Yb²⁺ crystals are also shown in Table 1. All samples exhibit similar values of about 540 ns, slightly shorter than 585 ns reported in Ref. 20, which proves no negative effects coming from Yb codoping on the Ti⁺ emission centers themselves. The photopeaks in pulse-height spectra were approximated by a gaussian to evaluate the peak position and to estimate the relative light yield (see supplemental data) of group A crystals. Relative light yield values under the 662 keV gamma excitation from ¹³⁷Cs are also listed in Table 1. At the lowest Yb co-doping concentration (0.005 mol%), the light yield shows approximately 2% loss compared to Yb-free CsI:Ti. For higher co-doping concentration of 0.05 mole%, the light yield loss is about 14%.

After further optimization of Ti⁺ and Yb²⁺ concentration, the composition with excellent scintillation performances has been obtained. Pulse height spectra of optimized group B crystals under ²²Na (511 keV) excitation are measured. The light outputs as a function of integration time for group B are shown in Fig. 2. When integration time is 4 μs, the light output for ST3, ST1 and ST4 is 3350, 4241, and 4510 p.e./MeV, respectively. Considering the EWQE of R1306 PMT at 550 nm the emission maximum of CsI:Ti⁺,Yb²⁺ and LCE, it is estimated that the light yield of the best Yb-codoped crystal (ST4) can reach 90,000±6000 photons/MeV. The light yield of ST1 sample is 85,000±5000 photons/MeV, which is still much higher than that of the Yb-free one (ST3) which is 67,000±4800 photons/MeV, close to the typical value 65,000 photons/MeV for CsI:Ti single crystal.^{2,21,22} On the basis of the Bartram-Lempicki model $L_R = 10^6 / (\beta \times E_g)$,²³ the number of photons per unit of absorbed energy (MeV) can be roughly estimated, where $E_g = 6.2$ eV²⁴ is the bandgap of CsI, the value of β is 1.5-1.8²⁵ for ionic halide compounds. Thus, the theoretical light yield L_R for CsI:Ti should be within 89,600-107,500 photons/MeV. It is evident that the light yield of the optimized CsI:Ti⁺,Yb²⁺ approaches its theoretical value. The reasons for the light yield improvement are not understood at this stage, and further experimental investigation is currently ongoing. The pulse height spectra of optimized CsI:Ti⁺,Yb²⁺ crystals (group B) under ²²Na excitation are presented in Fig. 3. The FWHM energy resolutions obtained for 511 keV γ -rays from the ²²Na source are 9.2%, 8.1% and 7.9% for ST3, ST1 and ST4, respectively, plotted in Fig. 3. Besides, its scintillation decay time is about 1.3 μs, close to 1.2 μs of Yb-free one (see Table 2).

Fig. 4 shows the afterglow profiles after the X-ray pulse excitation. It is found that the Yb-doped crystal with highest light yield value exhibits the lowest afterglow level of about 0.035% at 80 ms while the Yb-free sample shows of about 1.14% (see Table 2). Thus, simultaneous improvement of afterglow, light yield and energy resolution in the Yb-codoped CsI:Ti scintillator, reported for the first time, will pave the way to its application in the fast imaging techniques. We also note that, except the energy resolution, in the case of identical size the physical and other

scintillation performances of slightly hygroscopic CsI:Ti⁺,Yb²⁺ crystals are comparable to those of the ultra-efficient (quite hygroscopic) alkali earth iodide scintillator - SrI₂:Eu²⁺, see comparison in Table 2.

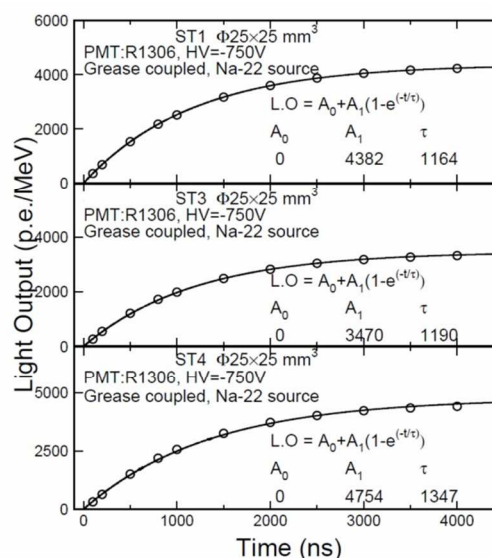


Fig. 2 Light output as a function of integration time for CsI:Ti⁺,Yb²⁺ group B crystals.

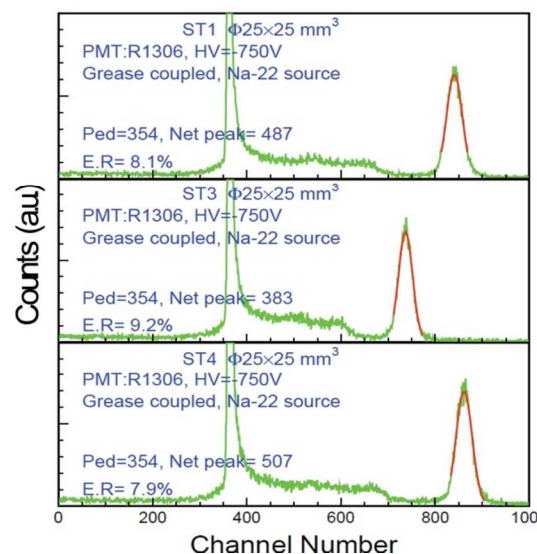


Fig. 3 Pulse height spectra of optimized CsI:Ti⁺,Yb²⁺ group B crystals coupled with Hamamatsu R1306 PMT under ²²Na excitation. Spectra start at channel no. 354, net photopeak position is marked in the figure, and solid red line is the Gaussian approximation of photopeak. The “net peak” equals the measured peak after subtracting the ADC pedestal signal. The equation, energy resolution (E.R.) = FWHM / Channel of “net peak”, is used to determine the energy resolution.

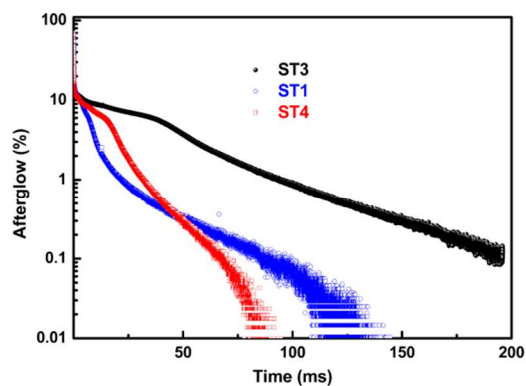


Fig. 4 Afterglow profiles of CsI:TI⁺, Yb²⁺ group B crystals after X-ray pulse excitation.

Fig. 5 presents the optical absorption spectra of group B crystals in the range of 300–800 nm. The abrupt absorbance increase below 330 nm is due to the onset of A-absorption band of TI⁺ center,²⁸ and there is no additional absorption band induced by Yb codoping, unlike in the case of Bi³⁺ codoping.^{15,16} An absence of the absorption features of the allowed Yb³⁺ related charge transfer (CT) transition, which should occur within 500–600 nm in iodides²⁹, implies that only the Yb²⁺ ions are stable in CsI host, which is also natural from the point of view of their charge compared to Cs⁺. The lowest 4f-5d₁ transition of Yb²⁺ should be situated around 400–420 nm in CsI host taking into account the similarity of 4f-5d transition positioning for Yb²⁺ and Eu²⁺¹⁷ and the position of Eu²⁺ 4f-5d₁ absorption band in CsI³⁰. However, due to strongly spin forbidden character of 4f-5d transition in Yb²⁺ it can be hardly observed in this concentration range³¹. Besides, in the Yb²⁺ codoped crystals, the apparent shift of TI⁺ absorption edge in codoped crystal was observed (inset of Fig. 5). We also recall the relative decrease of 400 nm shoulder in the emission spectra of Yb-codoped samples (Table 1) which can be due to nonradiative energy transfer from the TI⁺-like 400 nm band towards Yb²⁺ 4f-5d₁ absorption band or due to the change of the energy barrier for thermally stimulated transition from the 400 nm band towards the other co-existing exciton-like minima on the common adiabatic potential surface of the emission center excited state³². The observed changes in the absorption and emission characteristics of TI⁺ centers in the Yb-codoped crystals point to the spatial correlation between the Yb²⁺ and TI⁺ centers. In such a case the delayed migrating holes can be inhibited to reach TI⁰ being captured at Yb²⁺ ion in the vicinity. The return of Yb³⁺ + TI⁰ excited ion couple to the ground state can be easily nonradiative taking into account the well-known case of Ce³⁺ emission quenching in the Ce⁴⁺ and Yb²⁺ pairs e.g. in garnet³³ or oxyorthosilicate³⁴ materials.

Conclusions

In summary, positive role of Yb²⁺ codoping in the afterglow suppression in CsI:TI crystals was found. In the optimized composition, the CsI:TI⁺, Yb²⁺ crystal has so far exhibited an ultra-high light yield value of 90,000±6000 photons/MeV, energy resolution 7.9%@511 keV and suppressed afterglow level down to 0.035% at 80 ms. Simultaneous improvement of the afterglow

level, light yield and energy resolution in the Yb-codoped CsI:TI scintillator compared to standard CsI:TI one is considered as a breakthrough in the optimization of the scintillator and paves the way for its application in the X-ray fast imaging applications. The afterglow suppression in CsI:TI⁺, Yb²⁺ crystal is explained by spatial correlation of Yb²⁺ and TI⁺ ions where the former can trap the delayed migrating holes and inhibit their radiative recombination with TI⁰ counterpart.

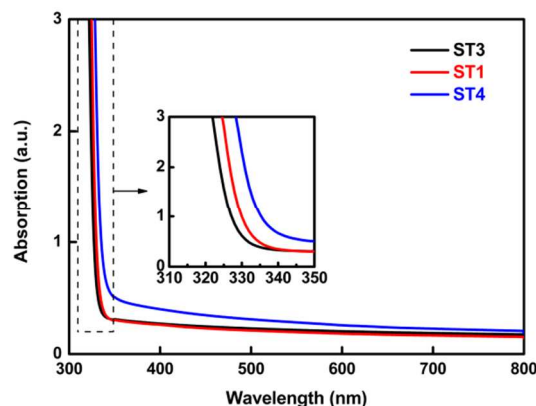


Fig. 5 Optical absorption spectra of optimized CsI:TI⁺, Yb²⁺ group B crystals. Parts of the spectra were enlarged for clear observation.

Acknowledgement

This work was supported by the National Natural Science Foundation of China (Grant No. 51372256). Partial support of the project of Sino-Czech collaboration funded by MEYS (Czech side), KONTAKT II, no. 12185 is also gratefully acknowledged.

Notes and references

- ^a Shanghai Institute of Ceramics, Chinese Academy of Sciences, No.215 Road, Jiading District, Shanghai, 201899, P.R. China. Fax: 86 21 59927184; Tel: 86 21 69987745; E-mail: caswyt@hotmail.com (Y.T. Wu), rgh@mail.sic.ac.cn (G.H. Ren)
- ^b Institute of Physics, Academy of Sciences of the Czech Republic, Cukrovarnická 10, 16253 Prague 6, Czech Republic.
- ^c California Institute of Technology, Pasadena, CA 91125, USA
- † Electronic Supplementary Information (ESI) available: [Optical absorption spectra and X-ray excited luminescence spectra data for CsI:TI group A crystals. Pulse height spectra data for CsI:TI group A crystals, when excited with a ¹³⁷Cs source].
- 1 W. Van Sciver, R. Hofstadter, *Phys. Rev.* 1951, **84**, 1062.
- 2 M. Nikl, *Meas. Sci. Technol.* 2006, **17**, R37.
- 3 B.K. Cha, J.H. Bae, C.H. Lee, S.H. Chang, G. Cho, *Nucl. Instr. Meth. Phys. Res. A* 2011, **633**, s297.
- 4 L.A. Kappers, R.H. Bartram, D.S. Hamilton, C. Brecher, A. Lempicki, V. Gaysinskiy, E.E. Ovechkina, V.V. Nagarkar, *Rad. Meas.* 2007, **42**, 537.
- 5 J.H. Siewersden, D.A. Jaffray, *Med. Phys.* 1999, **26**, 8.
- 6 S.C. Thacker, B. Singh, V. Gaysinskiy, E.E. Ovechkina, S.R. Miller, C. Brecher, V.V. Nagarkar, *Nucl. Instr. Meth. Phys. Res. A* 2009, **604**, 89.
- 7 P. Dorenbos, *J. Phys.: Condens. Matter* 1994, **6**, 4167.
- 8 K. Yang, C. L. Melcher, P. D. Rack, and L. A. Eriksson, *IEEE Trans. Nucl. Sci.* 2009, **56**, 2960.
- 9 J.J. Zhu, M. Gu, X.L. Liu, B. Liu, S.M. Huang, C. Ni, *J. Lumin.* 2013, **139**, 1.

- 10 N.G. Starzhinskiy, O. Sidletskiy, G. Tamulaitis, K.A. Katrunov, I.M. Zenya, Y.V. Malyukin, O.V. Viagin, A.A. Masalov, I.A. Rybalko, *IEEE Trans. Nucl. Sci.* 2013, **60(2)**, 1427.
- 11 C. Brecher, A. Lempicki, S.R. Miller, J. Glodo, E.E. Ovechkina, V. Gaysinskiy, V.V. Nagarkar, R.H. Bartram, *Nucl. Instru. Meth. Phys. Res. A* 2006, **558**, 450.
- 12 R.H. Bartram, L.A. Kappers, D.S. Hamilton, A. Lempicki, C. Brecher, J. Glodo, V. Gaysinskiy, E.E. Ovechkina, *Nucl. Instru. Meth. Phys. Res. A* 2006, **558**, 458.
- 10 13 V.V. Nagarkar, C. Brecher, E.E. Ovechkina, V. Gaysinskiy, S.R. Miller, S. Thacker, A. Lempicki, R.H. Bartram, *IEEE Trans. Nucl. Sci.* 2008, **55(3)**, 1270.
- 14 L.A. Kappers, R.H. Bartram, D.S. Hamilton, A. Lempicki, C. Brecher, V. Gaysinskiy, E.E. Ovechkina, S. Thacker, V.V. Nagarkar, *Rad. Meas.* 2010, **45**, 426.
- 15 D. Totsuka, T. Yanagida, Y. Fujimoto, Y. Yokota, F. Moretti, A. Vedda, A. Yoshikawa, *Appl. Phys. Exp.* 2012, **5**, 052601.
- 16 Y.T. Wu, G.H. Ren, X.F. Chen, D.Z. Ding, H.Y. Li, S.K. Pan, Submitted.
- 20 17 P. Dorenbos, *J. Phys.: Condens. Matter* 2003, **15**, 8417.
- 18 J.M. Spaeth, W. Msise, K.S. Song, *J. Phys. Condens. Matter* 1994, **6**, 3999.
- 19 C. Brecher, V.V. Nagarkar, V. Gaysinskiy, S.R. Miller, A. Lempicki, *Nucl. Instru. Meth. Phys. Res. A* 2005, **537**, 117.
- 25 20 M.M. Hamada, F.E. Costa, C.C. Pereira, S. Kubota, *IEEE Trans. Nucl. Sci.* 2011, **48(4)**, 1148.
- 21 M.J. Weber, *J. Lumin.* 2002, **100(1-4)**, 35.
- 22 C.W.E. Eijk, *Nucl. Instru. Meth. Phys. Res. A* 2003, **509(1-3)**, 17.
- 23 A.M. Srivastava, C.R. Ronda, *Luminescence: Theory and Applications*; Wiley-VCH: Weinheim, Germany, Chapter 5 (2007).
- 30 24 S.L. Molodtsov, A. Puschmann, C. Laubschat, G. Kaindl, V.K. Adamchuk, *Phys. Rev. B* 1991, **44(3)**, 1333.
- 25 P.A. Rodnyi, P. Dorenbos, C.W.E. van Eijk, *Phys. Stat. Sol. (b)* 1995, **187**, 15.
- 35 26 R. Hawrami, J. Glodo, K.S. Shah, N. Cherepy, S. Payne, A. Burger, L. Boatner, *J. Cryst. Growth* 2013, **379**, 63.
- 27 E.V. van Loef, K.S. Shah, J. Glodo, G.M. Wilson, US patent: US2010/0268074 A1 (2010).
- 28 S. Masunaga, I. Morita, M. Ishiguro, *J. Phys. Soc. Jpn.* 1966, **21**, 638.
- 40 29 M. Nikl, A. Yoshikawa, T. Fukuda, *Opt. Mater.* 2004, **26**, 545.
- 30 H.J. Seo, W.S. Zhang, T. Tsuboi, S.H. Doh, W.G. Lee, H.D. Kang, K.W. Jang, *J. Alloys Compounds* 2002, **344**, 268.
- 31 A. Bensalah, M. Nikl, E. Mihokova, N. Solovieva, A. Vedda, H. Sato, T. Fukuda, G. Boulon, *Rad. Meas.* 2004, **38**, 545.
- 45 32 V. Nagimi, A. Stolovich, S. Zazubovich, V. Zepelin, E. Mihokova, M. Nikl, G.P. Pazzi, L. Salvini, *J. Phys. Cond. Mat.* 1995, **7**, 3637.
- 33 N. Guerassimova, N. Garinier, C. Dujardin, A.G. Petrosyan, C. Pedrini, *Chem. Phys. Lett.* 2001, **339(3-4)**, 197.
- 34 D.W. Cooke, R.E. Muenchausen, B.L. Bennett, K.J. McClellan, A.M. Portis, *J. Lumin.* 1998, **79(3)** 185.

Table 1. Luminescence and scintillation characteristics of CsI:Ti⁺,Yb²⁺ group A crystals.

Sample	Tl concentration (mol%)		Yb concentration (mol%) In melt	PL decay constant ^a (ns)	Afterglow level @50 ms (%)	Relative light yield ^b (%)	RL integral intensity (%) ^c	RL relat. intensity at 400 nm ^d (%)
	In melt	In crystal						
IT1	0.078	0.010	0	540	0.490	100	100	18.6
IT2	0.078	0.011	0.005	525	0.041	98	90	14.0
IT3	0.078	0.012	0.05	543	0.041	86	76	8

^a Monitoring at $\lambda_{\text{ex}}=322$ nm and $\lambda_{\text{em}}=520$ nm.

^b Measured from the energy spectra under ¹³⁷Cs excitation.

^c Measured from the data of X-ray excited luminescence spectra.

^d RL intensity at the spectrum maximum is defined as 100%.

Table 2. Scintillation characteristics comparison between CsI:Ti⁺,Yb²⁺ (group B) and SrI₂:Eu²⁺ single crystals with the identical size.

Sample	Tl concentration (mol%)		Yb concentration (mol%) In melt	Scintillation decay constant ^a (ns)	Afterglow level (%)		Light yield ^a (photons/MeV)	Energy resolution @511eV (%)	Hygroscopic	Ref.
	In melt	In crystal			@50ms	@80ms				
SrI ₂ :Eu ²⁺	-	-	-	1000-5000 ^{b,c}	~0.20	~0.10	70000 - 11500 ^{b,c}	3.0 ^c	Very	[26,27]
CsI:Ti ⁺ (ST3)	0.156	0.039	0	1190	3.96	1.450	67,000±4800	9.2	Slight	This work
CsI:Ti ⁺ ,Yb ²⁺ (ST1)	0.156	0.031	0.005	1164	0.340	0.122	85,000±5000	8.1	Slight	This work
CsI:Ti ⁺ ,Yb ²⁺ (ST4)	0.234	0.070	0.005	1347	0.340	0.035	90,000±6000	7.9	Slight	This work

^a Excited under ²²Na with 511 keV.

^b Depend on Eu²⁺ concentration.

^c Excited under ¹³⁷Cs with 662 keV.